

SDRP Journal of Food Science &amp; Technology (ISSN: 2472-6419)

# Influence of Shear on the Gelation of Myofibrillar Protein Extracted from Humboldt Squid (*Dosidicus gigas*)

DOI: 10.25177/JFST.4.1.RA.442

Research

Received Date: 13<sup>th</sup> Dec 2018Accepted Date: 26<sup>th</sup> Dec 2018Published Date: 07<sup>th</sup> Jan 2019

Copy rights: © This is an Open access article distributed under the terms of International License.

**Weiwei Lin<sup>1</sup>, Xiuzheng Zhang<sup>1</sup>, Weichun Pan<sup>1,\*</sup>, Beijing Han<sup>1</sup>, Jiamei Fan<sup>1</sup>, Ang Li<sup>1</sup>**<sup>1</sup>Food Safety Key Laboratory of Zhejiang Province, The School of Food Science and Biotechnology, Zhejiang Gongshang University, Hangzhou, China 310018**CORRESPONDENCE AUTHOR**

Weichun Pan

Email: panweichun1@yahoo.com

**CITATION**Weichun Pan, Influence of Shear on the Gelation of Myofibrillar Protein Extracted from Humboldt Squid (*Dosidicus gigas*)(2019)SDRP Journal of Food Science & Technology 4(1)**ABSTRACT**

The effects of heat and shear at various pH and salt concentrations on the denaturation of myofibrillar protein extracted from Humboldt squid (*Dosidicus gigas*) are investigated. Squid tissues subjected to heating and simultaneous heating and shear force treatments differ in the extent of myofibrillar protein conformational change and composition. Gel formation processes differ in these two treatments, as determined by the complex viscosity ( $h^*$ ) measurement and light-scattering technique. Low-field nuclear magnetic resonance spectroscopy suggests shear promotes hydrophobic patch exposure during the gelation process to generate a product with high water content and compact structure. Shear-treated products therefore have large  $T_2$  values with small proportions compared with untreated products. A comparison of gelation and protein crystal nucleation suggests that protein gelation is driven by hydrophobic interactions.

**Keywords:** shear; myofibrillar protein gelation; *Humboldt squid*; structure; hydrophobic interactions

**INTRODUCTION**

In a moving fluid system, shear stress is incurred wherever a solid boundary exists. Given both the highly sensitive nature of protein molecules to their physicochemical environment, and the pervasive existence of shear stress, the influence of shear stress on protein molecule stability has been studied extensively. The pharmaceutical industry is particularly interested in the effects of shear stress on protein molecule stability, given denaturation might influence the shelf-life of protein pharmaceuticals, and maybe even cause clinical side-effects [1-2].

Contradictory accounts of the influence of shear stress on protein molecule stability exist. The mechanical energy contributed by shear stress should be comparable to heat energy to observe lysozyme molecule denaturation [3]. However, Ashton et. al. [4] found shear stress to be 3 orders of magnitude smaller to repetition the same effect, a result also reported by Byington et. al. [5-6]. In rheological assessments the phenomena of lysozyme reversible conformation change [7] and cluster formation [5] suggests some

conformations could be created only via shear treatments. In addition, some conformations can be generated only by shear treatment, endowing a gel with textural properties not otherwise obtained by heating. This stems from the fact that the pattern of exposed residues is dictated by molecular conformation and regulates the bond-formation between neighbor protein molecules in the gelation process, thereby determining a gel's textural properties.

This work is inspired by the result of Charm and Lai [8], which state the parameter of  $\dot{\gamma}^\theta$  ( $\dot{\gamma}$  the shear rate and  $\theta$  the time of exposure) instead of  $\dot{\gamma}$  or/and  $\theta$  governing protein molecule conformation change when shear field exists. It is common in food industry that the shear rate could be small but the exposure time could be long. As a result, the product of  $\dot{\gamma}^\theta$  could be comparative to the value reported in above-mentioned literature. But since the traditional wisdom in food industry usually focuses on the shear rate, its influence on protein conformation is ignored.

The second motivation comes from the fact that non-globular protein molecules are pervasive in food and have an innate asymmetrical geometrical structure, giving them an orientational preference in a shear field [2]. Bond-formation in the gelation process is also orientational. Therefore, the introduction of a shear field could be used to influence the protein gelation process. A large gel size might also generate remarkable tensile force, exacerbating conformation change due to a shear field [9].

Whether the influences generated by the shear field occur in protein gels is not well studied [10]. On the other hand, the results presented in Fig S1 revealed the potential of this technique to regulate myofibrillar protein gelation extracted from Humboldt squid.

We studied myofibrillar proteins of Humboldt squid for two reasons: 1) their physical properties are well-known, and 2) this squid is abundant and highly nutritious [11]. Unfortunately, without pretreatment,

Humboldt squid tissues are bitter, and their proteins highly soluble, limiting demand for consumption [12]. Application of a chemical (like sodium carbonate ( $\text{Na}_2\text{CO}_3$ )) to the flesh removes bitterness, increasing the potential for use of this squid as a raw material for surimi, once its poor gelation properties are overcome [13-14].

## 2. MATERIALS AND METHODS

As pH and salt concentration can significantly influence interactions between protein molecules and molecular conformation [15], a pH range of 5.5–9.5 (covering the isoelectric point (pI) of the myofibrillar proteins) and potassium chloride (KCl) as a salt at concentrations 0.1, 0.5 and 0.9 M were applied in this study.

Solutions were subjected to three treatments: 1) controls (without treatment); 2) heating only (a traditional gelation process); and 3) simultaneous heating and shearing (HS).

### 2.1. Raw materials

Humboldt Squid, caught and immediately frozen at  $-20^\circ\text{C}$ , were obtained from the Zhoushan Second Marine Fisheries Company in Zhejiang, China. Within three months of collection squid (usually four of average mantle length 1 m) were defrosted at room temperature, deheaded, gutted, and cleaned using water. Mantle and fin tissues were bagged and stored at  $-80^\circ\text{C}$  for further experiments.

Reagent grade  $\text{Na}_2\text{HPO}_4$ ,  $\text{KH}_2\text{PO}_4$ , KCl,  $\text{CH}_3\text{CH}_2\text{OH}$ , and  $\text{CH}_3\text{COOH}$  were provided by Huipu Inc. (Hangzhou, China). All other reagent grade chemicals were purchased from Sigma (St. Louis, MO, USA).

### 2.2. Gel formation

Mixtures containing a pellet of myofibrillar protein extracted from squid (procedure detailed in Supporting information) and a KCl solution of the appropriate pH in a 1:2 weight ratio were prepared for gel formation. The solutions were left to stand for 3 h for

maximum protein dissolution.

Myofibrillar protein gels were prepared using two methods. The first comprised three consecutive steps: heating the solution at 40°C for 60 min, then at 90°C for 30 min, before cooling to 0°C for 30 min. The solution was refrigerated overnight before being centrifuged at 2000 × *g* for 10 min at 4°C, after which the supernatant and sediment were collected. All procedures occurred in a parafilm-covered 100 mL beaker to prevent water loss during heating.

In the second method, the protein gel was created using a rheometer (MCR 302, Anton Paar GmbH, Graz, Austria) with a concentric cylinder system (CC50), at operating parameters 0.3% strain (in the region of linear elasticity) and 1 Hz, after which the solution was transferred to a 100 mL beaker and cooled to 0°C for 30 min. Other procedures were as described for heating gelation.

In both methods, water temperature was maintained using a water tank connected to a refrigerated/heating circulator (F12-MA, Julabo GmbH, Seelbach, Germany). The cooling procedure was similar as the heating gelation.

### 2.3. Circular dichroism (CD) analyses

CD spectra were recorded in the far-UV range (250–190 nm) using a CD spectropolarimeter (J-815, Jasco Corp., Tokyo, Japan) and a 0.1-cm quartz CD cuvette at 25 °C. The protein concentration for analysis was maintained at 50 μg mL<sup>-1</sup> for all samples; the corresponding solutions without protein were used as blank buffers. The scan rate, response, bandwidth, and sensitivity were set at 50 nm min<sup>-1</sup>, 0.25 s, 1.0 nm, and 0.1°, respectively. Each spectrum was recorded in triplicate. The percentages of α-helix, β-sheet, β-turn, and random coil structures were assessed using the protein secondary structure estimation program provided with the Jasco J-815 spectropolarimeter [16].

### 2.4. SDS-PAGE

PAGE using dissociating SDS and a Tris–glycine–SDS buffer system in a continuous gel (from 6% to 18%) was performed as described by Laemmli [17] using a Mini-Protean™ Tetra system (Bio-Rad Laboratories, Richmond, CA, USA). All proteins were analyzed using their electrophoretic protein patterns. Samples were subjected to a dissociating system containing 0.1 M Tris–HCl, 4% SDS (w/v), 20% glycerol (v/v), 5 × 10<sup>-5</sup> bromophenol blue (3',3'',5',5''-tetrabromophenolsulfonephthalein, w/v), and 200 mM dithiothreitol, denatured by heating at 100 °C for 5 min and then cooling to room temperature (~20 °C) before loading. The loading sample concentration was 2 mg mL<sup>-1</sup>. The electrophoretic runs were performed at 17–25 °C for half an hour at 70 V, then 3 h at 110 V. A broad range of molecular weight protein standard solutions were used (Bio-Rad Laboratories), namely myosin (200 kDa), β-galactosidase (116 kDa), phosphorylase b (97.2 kDa), bovine serum albumin (66.4 kDa), ovalbumin (44.3 kDa), carbonic anhydrase (29 kDa), trypsin inhibitor (20.1 kDa), lysozyme (14.3 kDa), and bovine aprotinin (6.5 kDa). After electrophoresis, the gel was stained with 0.1% (w/v) Coomassie Brilliant Blue R-250 (Bio Basic Inc., Markham, Canada) in 40% ethanol and 10% acetic acid and then destained with 40% (v/v) ethanol and 10% acetic acid. The patterns of the constituents of the myofibrillar proteins at various pH values and salt concentrations were analyzed with Quantity One software (Bio-Rad) using a computer with a scanner (GS800, Bio-Rad).

### 2.5. Theory of light scattering

For static light scattering (SLS) (since particle size is close to the wavelength of the detecting light), Zimm plots were used to determine the intermolecular interactions, the second virial coefficient *A*<sub>2</sub>, and the radius of gyration *R*<sub>g</sub> in accordance with Zimm [18]:

$$\frac{Kc}{R} = \frac{1}{M_w} \left( 1 + \frac{q^2 R_g^2}{3} \right) + 2A_2 c \quad (1)$$

where: *K* is a system constant defined as  $k = \frac{(2\pi n_0/\lambda^2)^2}{N_A} \left( \frac{dn}{dc} \right)^2$  [19], in which *n*<sub>0</sub> is the refractive index of the solvent, ~ 1.3342, 1.3383 and 1.3424 for

0.1 M, 0.5 M and 0.9 M KCl solutions, respectively [20];  $l$  is the wavelength of laser light, 632.8 nm;  $N_A$  is Avogadro's number;  $dn/dc$  is the derivative of the refractive index  $n$  with respect to solution mass concentration;  $M_w$  is the molecular weight of the solute molecule; and  $q$  is the scattering wave vector,  $= 4\pi n_0 \sin(\theta/2) / \lambda$ , where  $q$  is the angle of the detector.

For dynamic light scattering (DLS), the correlation function of the light scattering intensity  $g_2(t)$  was expressed after Pan et al. [21]:

$$g_2(t) - 1 = (D_1 e^{-t/\tau_1} + D_2 e^{-t/\tau_2})^2 + \varepsilon \quad (2)$$

where:  $D$  is the amplitude of light intensity;  $t$  is the characteristic time of the diffusion of the scatterer, determined by numerically inverting the Laplace transform of  $(g_2(\tau) - 1)^{1/2}$  with the aid of the software package provided by ALV-GmbH based on CONTIN algorithm [22-23]; and  $\varepsilon$  is noise. Based on the Stokes-Einstein relation, the equivalent hydrodynamic radius  $R_H$  could be estimated by:

$$R_H = \frac{k_B T q^2}{6\pi\eta} \tau \quad (3)$$

where  $\eta$  is the viscosity of solvent in the measured solution.

Light-scattering was performed using the ALV/CGS-3 goniometer (ALV, Langen, Germany) with a He-Ne laser. Refractive index increments were determined by a SEC-3010 DN/DC differential refractometer (WGE Dr. Bures, Dallgow-Doberitz, Germany), operating at 620 nm wavelength and 25°C.

For SLS measurement, sample concentrations ranged from 0.1 to 1 mg mL<sup>-1</sup> to maintain a single phase and monomeric protein in the solution. Measurement angles varied from 15–90° in 5° increments. Data were analyzed using software provided by the ALV Company.

For DLS determination, a protein solution of concentration 1 mg mL<sup>-1</sup> was prepared. To eliminate dust or air bubbles, supernatants from samples centrifuged at

5000 ×  $g$  for 15 min at 4°C were collected. Each DLS measurement was performed at 25°C, a measurement angle of 90° at acquisition time of 1 min; measurements were performed in triplicate.

## 2.6. Apparent viscosity measurement during protein gelation

The saturated myofibrillar protein solution at pH 7.5 and KCl 0.1 M (similar to the actual surimi process) was used to record apparent viscosity via the MCR 302 rheometer with a concentric cylinder system (CC50) during gelation. Heating rates were 1°C min<sup>-1</sup> and 5°C min<sup>-1</sup>; shear rates were 0.1s<sup>-1</sup>, 1s<sup>-1</sup> and 10s<sup>-1</sup>; the temperature range was 20–90°C. Each sample was tested in triplicate.

## 2.7. Water-holding capacity (WHC)

The WHC of gels was determined using a modified version of Kuhn and Foegeding [24]. Gels were cut with a metal cork borer to obtain cylindrical samples of height 1 cm and diameter 1 cm. Before centrifugation, tube weight with and without core samples was determined by balance (ME204E, Mettler-Toledo LLC., Columbus, OH). Core samples were then inserted into centrifugal filtration units (Changsheng Biotech. Co., Hangzhou, China) and spun at 10000 ×  $g$  for 10 min at 4°C. After removal of expelled fluid, samples were reweighed. Each gel was tested in triplicate; the WHC of each was determined according to:

$$WHC = \frac{W_1 - W}{W_2 - W} \times 100\% \quad (4)$$

where  $W$  represents the weight of the centrifugation tube, and  $W_1$  and  $W_2$  are the weights of the tube with gel before and after centrifugation, respectively. Each sample was tested in triplicate.

## 2.8. Low-field nuclear magnetic resonance (LF-NMR) measurements

We used an NMR analyzer (PQ 001, Niumag Co., Ltd., Shanghai, China) for LF-NMR measurements. Samples (5.0 g) were placed in NMR glass tubes of diameter 60 mm.  $T_2$  relaxation times were measured

using the Carr-Purcell and Meiboom-Gill sequence.  $T_2$  measurements were performed using a  $t$  value of 400ms (time between  $90^\circ$  and  $180^\circ$  pulses). Data from 1200 echoes were acquired as 32 scan repetitions, with a 1 s repetition time between successive scans, with all measurements made within 2 min. These steps were repeated four times at  $25^\circ\text{C}$ . The data were analyzed using MultiExp Inv. analysis software (Niumag Co., Ltd., Shanghai, China) by fitting a curve to the continuous distribution of exponentials using the following:

$$R_{\text{mag}}(t) = \sum_{j=0}^p P_{2j} \exp\left(-\frac{t}{T_{2j}}\right) + e(t) \quad (5)$$

where:  $R_{\text{mag}}$ , represents the total magnetization signal from the sample;  $P_{2j}$  and  $T_{2j}$  represent the spin-spin relaxation amplitude and time, respectively, of the  $j$ th fraction; and  $e(t)$  represents the residual error. Each sample was tested in triplicate.

The  $T_{20}$  value is the relaxation time of water molecules at 1–10 ms, and indicates whether water molecules are closely associated with macromolecules;  $T_{21}$  is the relaxation time of water molecules at 30–60 ms, and identifies whether water molecules are trapped in highly organized protein structures such as tertiary or quaternary structures; and  $T_{22}$  is the relaxation time of water molecules at 100–400 ms, and indicates whether water molecules are highly mobile and occur within large pores of the gel [25–26].

The  $T_{20}$  value suggests weak interactions between water molecules and surrounding macromolecules, the  $T_{21}$  value reveals that large spaces exist to host these water molecules, and the  $T_{22}$  value reveals the corresponding water molecules can be easily removed from the gel.

## 2.9. Statistical analysis

One-way analysis of variance was used to determine the significance of any differences between means, followed by Duncan's multiple-range test, using SPSS version 20.0 (IBM, USA).

## 3. Results and discussion

### 3.1. Effect of shear on molecular conformation

Since there is a remarkable molecular conformation change when salt concentration shifts from 0.1 M to 0.5M but no further changes occurs when salt concentrated to 0.9 M, the range of salt concentration in this study was defined from 0.1 M – 0.9 M [15].

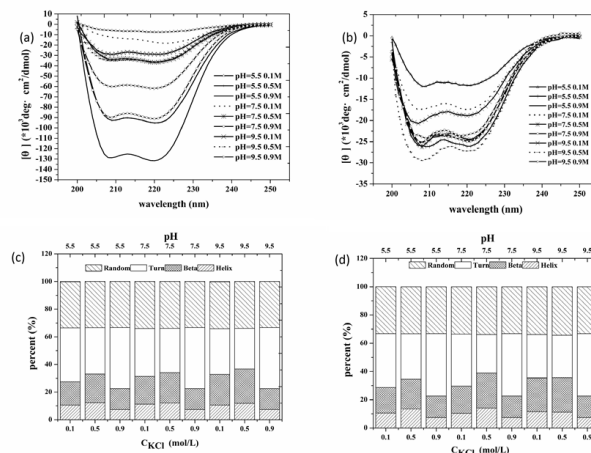


**Figure 1.** Effects of shear treatment during myofibrillar protein gelation on protein molecule secondary structure. (a) and (b) are CD spectrums of myofibrillar protein with the absence of (a) and the presence of shear treatment (b) respectively, while (c) and (d) the corresponding secondary structure distributions.

The protein conformational changes caused by pH and KCl variations were supported by CD analysis. Fig. 1a and 1b show that  $[q]$  in samples via heating gelation is larger than that in HSs, which may come from the fact that solutions of heating gelation contains more soluble proteins than HS solutions (Fig. S2). Spectral shifts due to shear cause change in the distributions of secondary structures (Fig. 1c and 1d). Shear treatment at pH 5.5 and low salt concentrations (0.1 M, 0.5 M) increased the  $\alpha$ -helix and  $\beta$ -sheet contents, whereas at 0.9 M KCl, only the  $\beta$ -sheet content increased. Furthermore, all changes occurred at the cost of turn content, suggesting that shear treatment favored regular protein conformations at low pH (5.5).  $\alpha$ -helix content increase due to shear treatment is astounding since shear treatment favors the stable secondary structure,  $\beta$ -sheet, and against  $\alpha$ -helix [27–28]. This odd phenomenon may come from the cova-

lent bond formation between neighbor protein molecules, which could benefit  $\alpha$ -helix survive during gelation process. Since protein molecule position distribution in solution remarkably modifies with shear induction, the patterns of covalent bond formation between neighbor protein molecules vary significantly as well.

At a KCl concentration of 0.1 M, a similar trend is observed at pH 7.5; the distributions of myofibrillar protein secondary structures are the same in samples via heat treatment and HS. At 0.1 M KCl and pH 9.5, there is no change in the secondary structure distribution. However, at 0.5 M KCl, the  $\beta$ -sheet content increased and that of  $\alpha$ -helices decreased; the contents of the other two structures are similar to those at 0.1 M KCl. At 0.9 M KCl, opposite changes are obtained, with the contents of turn and random structures being same as those in 0.5 M KCl solutions.

Not only does shear affect the secondary structure distribution of a protein, it affects its composition in solution also. Fig. 2 reveals that heating created new protein species of low molecular weight at the cost of myosin heavy chain (MHC) and heavy meromyosin (HMM) proteins, such as those above actin in the SDS-PAGE electrophoresis patterns in samples via heating gelation and HS, respectively. This implies molecular degradation of MHC and of HMM during heating. HS contains more tropomyosin but less myosin light chain (MLC) than solutions of heating gelation.

### 3.2. Effects of shear on intermolecular interactions

Since the intermolecular interactions regulate the phase transitions in solutions [29-30], it is worth to investigate the shear influence on these properties. Meanwhile, the state of individual protein and its time evolution in gel are other key facts to determine the gel properties but are hard to be accessed by current techniques. Regarding to this question, the fluorescence spectroscopy is a promise solution [31]. However myofibril contains at least 10 species of protein (Fig. 2). It is almost impossible to distinguish

molecular conformation changes of each protein species via fluorescence signals. Although the gene engineering could solve this question via plugging the special fluorescence residue in the amino acid sequence of target protein molecule, this procedure is very difficult and the new residue could complicate the study since its influence on the properties of host molecule needs to be assessed. The alternative way is to probe protein molecules and its aggregators in co-existing solution of gel. The philosophy behind this is that all protein species in solution are equilibrium to gel thermodynamically. Thus, the properties of these species could be used to estimate the ones to construct gel, and thereby to assess the thermodynamic properties of gel, key information to control gelation process.

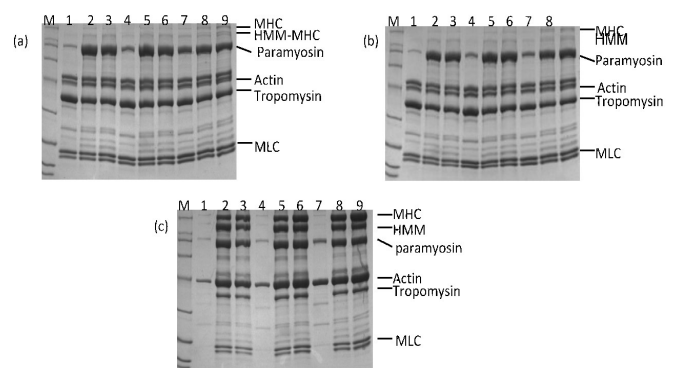


**Figure 2.** SDS-PAGE electrophoresis analyses of supernatants after myofibrillar protein gelation (a) without and (b) with shear treatment; M indicates markers. Bands 1–3 represent solutions of pH 5.5 and KCl concentrations from 0.1 M to 0.9 M with a step of 0.4 M. Bands 4–6 represent solutions of pH 7.5 and the same order of KCl concentrations as for bands 1–3. Bands 7–9 represent solutions the same as those for 1–6, except at pH 9.5. (c) Untreated reference solution.

Fig. 3 shows that intermolecular interactions, characterized by the second virial coefficient  $A_2$ , are affected by the pH and KCl concentration. For control solutions,  $A_2$  increased with salt concentrated until it attained to 0.5 M. However salt with further increase did not affect  $A_2$ . This complex salt concentration dependency of intermolecular interactions comes

from two facts, 1) the double-layer force via tune the Debye-length modification, and 2) protein molecule conformation change. But in high salt concentration region ( $>0.5$  M), both facts would be almost independent of salt concentration [15]. In addition, in this high salt concentration range,  $A_2$  is independent of pH, which is contrast to low salt concentration (0.1 M) in which  $A_2$  reduces with pH enhancement. This is due to protein molecule conformation modification by pH [32].

In heating gelation experiments, at pH 5.5,  $A_2$  increased slightly as KCl concentration increased from 0.1 to 0.9 M. In contrast, at pH 9.5,  $A_2$  kept increase with salt concentrated throughout the whole study range. The interest phenomenon occurred at pH 7.5, in which  $A_2$  attained maximal at 0.5 M KCl (Fig. 3). On the other hand, pH influence depends on salt concentration as well. In 0.1 M KCl solutions,  $A_2$  attained minimal at pH 7.5. With salt concentration further rising to 0.5 M,  $A_2$  increased and eventually saturated with pH rising. In 0.9 M KCl solutions, the local minimum appeared at pH 7.5 while the maximum value presented at pH 9.5. This complicate picture of  $A_2$  dependency on salt concentration and pH indicates that these two parameters have dramatic influence on myofibrillar protein gelation process and thus are promise means to tune gel properties.

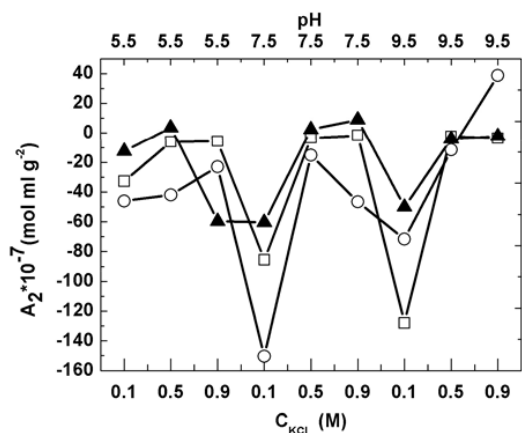


**Figure 3.** Static light-scattering measurements for second virial coefficient, in myofibrillar solutions subject to three types of treatment: control (open squares), heating gelation (open circles), and HS (solid triangles).

It is noticed that  $A_{2S}$  in control solutions has uncorrelation with the ones in heating gelation solutions. This observation hints the complexity of myofibrillar gelation process. The slight change at initial solutions, no matter solution conditions or protein molecule conformation, could cause the unpredictable and remarkable difference in the final solutions during this process, which is one factor to endow food research as art rather than science and is due to the existence of multiply-step reactions, generally speaking, including two steps, protein molecule unfolding and then bond formation between protein molecules [33]. In principle, the variation of intermolecular interactions is able to affect the collision of protein molecules in solution [34] and thereby affect the pattern of bond formation between protein molecules in gel. The existence of protein molecule conformation change due to the surrounding solution condition modification even exacerbates the complexity of protein gelation process. Caveat: protein molecule conformation variation always associates with intermolecular interactions change. Thus, it is hard to investigate the conformation change effect alone in gelation process. Due to the two-fold effect of salt concentration, it is pervasive that salt concentration is widely utilized to optimize protein process [35-36].

The second issue contributing to this uncorrelation phenomenon is the myofibrillar protein composition variation (Fig. 2) because

$$A_2^{no} = \frac{1}{2(\langle M_w \rangle^{no})^2} \sum_{i,k=1}^n f_i f_k M_w^k M_w^i A_2^{ik} \quad (6)$$

where the subscript  $k$  and superscript  $k$  denote species  $k$ ;  $f$  is the weight fraction,  $M_w$  is the molecular weight,  $A_2^{jk}$  is the second virial coefficient between species  $j$  and  $k$  [37]. So far, we are unable to identify which issue dominates this uncorrelation phenomenon!

In HS experiments, the pattern of  $A_2$  dependency on salt concentration at fixed pH from 5.5 to 9.5 with 2 steps shifted from the local maximum, to strictly monotonic increase and then to increase to a saturate value (Fig. 3). In contrast, the pattern of  $A_2$  depend-

ency on pH changed from the local minimum, to the almost constant value and then to increase to a saturated value.

Furthermore, at low salt concentration range ( $\leq 0.5$  M),  $A_2s$  in HS are always larger than the ones in control solutions and solutions of heating gelation. In other words, heat and shear treatment in myofibrillar protein solutions reduces the attraction force between molecules. Since the strong attraction force between protein molecules leads to less solubility [29], while one barrier for Humboldt squid application in surimi industry is the high solubility of its protein [12], shear indeed deteriorates Humboldt squid application in this salt concentration range. However, at 0.9 M, except pH 7.5,  $A_2$  obtained in HS was less than the one in solutions via heating gelation.

And the uncorrelation of  $A_2s$  obtained in three types of solutions with same salt concentration and pH suggests that shear indeed plays a role in myofibrillar protein gelation via modifying not only protein molecule collision during gelation but also its unfolding process, supported by Fig. 1.

### 3.3. Effects of shear on aggregators

In gelation, a 3D structure nucleates and grows consecutively; therefore the solution equilibrium with gels should have intermediate products which are named by aggregators. The apparent molecular weight and geometrical information (Fig. 4 and Table 1), quantified by the radius of gyration and the hydrodynamic radius, of aggregators provide an avenue to investigate the protein gelation process.

A control solution contains aggregators with the radius of gyration fluctuating around 100 nm (Fig. 4a), but the corresponding apparent molecular weights vary by about two orders of magnitude (Fig. 4b). At pH 5.5 and 7.5, molecular weight increased with salt concentration increasing, whereas at pH 9.5, a maximum value appeared at 0.5 M KCl. On the other hand, the pattern of molecular weight dependency on

pH shifts from a concave function, to a monotonic one and eventually to a convex one. This observation indicates that an aggregator becomes compact with salt concentrated when pH fixed and is due to the enhancement of screening-effect [38]. The compactness of aggregators could be estimated by the value of  $M_w/R_g^3$  as well (Table 2). This value at pH 5.5 is larger than the ones at pH 7.5 and 9.5.

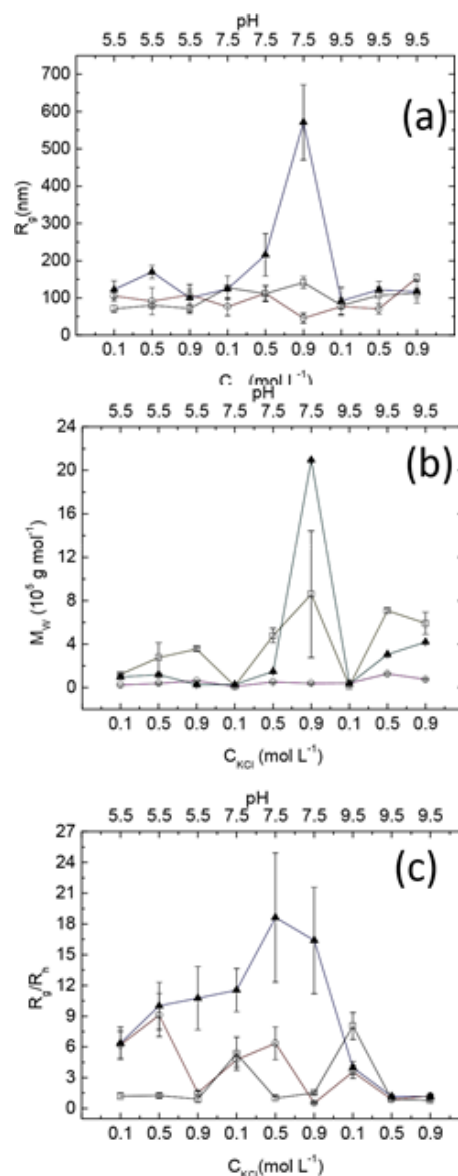


**Figure 4.** Static light-scattering measurements for the radius of gyration (a), molecular weight (b), and  $R_g/R_H$  ratios(c), in myofibrillar solutions subject to three types of treatment: control (open squares), heating gelation (open circles), and HS (solid triangles).

**Table 1:** Dynamic light-scattering results for myofibrillar solutions. Each set of two rows contains the decay time (the upper row) and the corresponding light-intensity percentage (the bottom row). NS denotes the initial untreated myofibrillar solution; ST denotes the supernatant of the heat-treated myofibrillar solution, and SHT denotes the gelation solution subjected to simultaneous heating and shearing.

pH C <sub>KCl</sub> (M)	5.5			7.5			9.5			
	0.1	0.5	0.9	0.1	0.5	0.9	0.1	0.5	0.9	
Decay time (ms) & light intensity percentage	NS	0.77±0.12 <sup>ax</sup> 99.5%	0.83±0.12 <sup>ax</sup> 99.0%	1.03±0.25 <sup>ay</sup> 99.7%	0.31±0.17 <sup>ax</sup> 99.3%	1.45±0.43 <sup>ay</sup> 80.1%	1.20±0.41 <sup>ay</sup> 97.0%	0.13±0.11 <sup>ax</sup> 64.2%	1.57±1.01 <sup>ay</sup> 65.5%	1.88±0.67 <sup>ay</sup> 80.2%
	ST	0.22±0.09 <sup>bx</sup> 98.7%	0.13±0.10 <sup>bx</sup> 59.2%	0.93±0.42 <sup>ay</sup> 59.0%	0.21±0.06 <sup>ax</sup> 99.3%	0.23±0.09 <sup>bx</sup> 99.1%	1.10±0.83 <sup>ay</sup> 57.6%	0.28±0.14 <sup>bx</sup> 99.8%	1.04±0.79 <sup>ay</sup> 84.3%	1.67±0.44 <sup>ay</sup> 89.5%
	SHT	0.25±0.11 <sup>bx</sup> 99.2%	0.22±0.10 <sup>cx</sup> 97.5%	0.12±0.05 <sup>bx</sup> 88.3%	0.14±0.10 <sup>ax</sup> 50.9%	0.15±0.14 <sup>bx</sup> 67.4%	0.45±0.20 <sup>bx</sup> 99.5%	0.30±0.15 <sup>bx</sup> 99.1%	1.36±0.96 <sup>ay</sup> 86.5%	1.31±0.79 <sup>ay</sup> 89.3%

<sup>a-c</sup> Within columns, means with different superscripts are significantly different ( $p < 0.01$ ).

<sup>x-y</sup> Within rows of pH value, means with different superscripts are significantly different ( $p < 0.01$ ).

**Table 2:** The value of  $M_w/R_g^3$

pH C <sub>KCl</sub> (M)	5.5			7.5			9.5		
	0.1	0.5	0.9	0.1	0.5	0.9	0.1	0.5	0.9
NS	0.34±0.12 <sup>ax</sup>	0.53±0.36 <sup>ax</sup>	0.98±0.21 <sup>ay</sup>	0.01±0.01 <sup>az</sup>	0.34±0.13 <sup>au</sup>	0.3±0.21 <sup>au</sup>	0.02±0.02 <sup>av</sup>	0.36±0.09 <sup>aw</sup>	0.42±0.11 <sup>aw</sup>
ST	0.02±0.02 <sup>bx</sup>	0.05±0.03 <sup>bx</sup>	0.05±0.03 <sup>bx</sup>	0.03±0.03 <sup>ax</sup>	0.04±0.02 <sup>bx</sup>	0.41±0.26 <sup>ay</sup>	0.09±0.05 <sup>bz</sup>	0.36±0.16 <sup>ax</sup>	0.02±0.02 <sup>by</sup>
SHT	0.05±0.04 <sup>bx</sup>	0.02±0.02 <sup>bx</sup>	0.03±0.03 <sup>bx</sup>	0.01±0.01 <sup>ax</sup>	0.01±0.01 <sup>bx</sup>	0.01±0.01 <sup>bx</sup>	0.04±0.02 <sup>bx</sup>	0.17±0.09 <sup>by</sup>	0.26±0.12 <sup>cy</sup>

<sup>a-b</sup> Within each pair (ST vs. SHT), means with different superscripts are significantly different ( $p < 0.01$ ).

<sup>u-z</sup> Within columns, means with different superscripts are significantly different ( $p < 0.01$ ).

On the other hand, when salt concentration is low (0.1 M), pH change causes charge redistribution around the aggregator surface. Since pH 7.5 close to pI of myofibrillar protein of Humboldt squid, the net charge number an aggregator carrying could decrease and follows up with increase when pH shifts from 5.5 to 7.5 and then to 9.5. The corresponding repulsive interactions among aggregators should have the same trend. And compared with pH 9.5, pI of myofibrillar protein closes to pH 5.5. Thus, based on the above-mentioned observation, when pH shifting from 7.5 to 5.5 and then to 9.5, an aggregator become more and more loss with salt concentration maintaining constant.

Unlike the gyration radius, the corresponding hydrodynamic radius of aggregator in myofibrillar protein solutions (Table 1), which is proportional to the decay time ( $R_H = \frac{k_B T q^2}{6\pi\eta} \tau$ ), demonstrated a distinct pattern of salt and pH dependence. Generally, the hydrodynamic radii of aggregators of control solutions are larger than the ones in solutions of heating gelation and HS. However, the relative position of this value in solutions of heating gelation and HS solutions varies with various pH and salt conditions. This observation reveals that the size of particle is a collective effect of salt concentration, pH and flow field.

In control solutions, generally, with salt concentrated, the hydrodynamic radius increases at each pH value, which could be the consequence of “screening effect” enhancement to reduce the repulsive double-layer force [39]. The other reason behind this phenomenon may be due to salting-in effect [40], a similar behavior observed in globular protein solutions [21, 41]. In contrast, the pH dependency of hydrodynamic radius is complex. In 0.1 M salt solutions, an aggregator shrank due to pH rising, opposite to the trend occurred in 0.5 M and 0.9 M salt solutions.

The traditional theory states that pH regulates the charge distribution around protein molecules and thereby determines the value of net charge protein molecule carrying [42]. On the other hand, salt concentration could modify the Debye-length and thereby influence the double-layer force. But muscle protein molecules distinguish from the abovementioned case and could be suffered conformation change when pH and salt concentration vary [43], which complicates the study of protein gelation process.

On the other hand, heating gelation solutions with high salt concentration (0.9 M) always preferred to contain larger size of aggregators. However, the difference of hydrodynamic radii of aggregator in HS solutions becomes less significant ( $p > 0.01$ ). Only at pH 9.5 the similar behaviors appears as the one in heating gelation solutions. In other pH values, no obvious ( $p > 0.01$ ) hydrodynamic radii difference occurred. Furthermore, the influence of pH on the hydrodynamic radius was not obvious ( $p > 0.01$ ) as well. This observation strongly implies three aspects. 1) Heating process not only denatures protein molecules but also dissolves aggregators. This dissolution process could come from high solubility of itself due to temperature change and/or single molecule denaturation, in which the bond to maintain a protein molecule attachment to an aggregator is broken with this protein molecule leaving to solutions. So far, it is not possible to evaluate which one dominates this size shrinking process. 2) One of the shear influences on gelation is the reduction of the size of aggregator, which could ascribe to the acceleration of protein

molecule dissolution from aggregator in heating process with the presence of flow field. And the second potential mechanism is the collective effect of shear and heating to speed up protein molecule denaturation process compared with heating alone. But the difference between these two types of solutions (heating gelation and HS) has low possibility of occurrence, only at 0.9 M salt with pH 5.5 and 7.5, which is reasonable since the extra energy input due to shear is small ( $\sim 10^{-3}$ ) compared with heating energy [4]. 3) Both salt concentration and pH are able to affect intermolecular interactions and molecular conformation as well. However, regarding to hydrodynamic radius assessment, salt concentration has small influence on aggregator than pH during heating gelation, which could stem from the modification of charge distribution along the aggregator surface and thus affect the stability of bonds between individual molecules and/or even between the one along aggregator surface and the other residing the layer next inside surface. Salt concentration could play the same role as pH doing but at less extent.

Furthermore, except (pH 7.5, 0.9 M) and (pH 9.5, 0.5 M), the values of  $M_w/R_g^2$  in solutions of heating gelation are much less than the ones in control solutions, which suggests that heating may cause aggregator dissolution with the pattern of pH and salt concentration dependencies. The shape of aggregator in solutions of heating gelation is different from the one in control solutions as well via the ratio of  $R_g/R_h$  (Fig. 4c). In control solutions, except (pH 7.5, 0.1 M) and (pH 9.5, 0.1 M), the geometrical shapes of aggregator are close to spherical. On the other hand, the geometrical shapes of aggregator in solutions of heating gelation depend on detail solution conditions. At pH 5.5, when salt concentration was lower than 0.5 M, aggregators presented as a rod ( $R_g/R_h > 2$ ) [44], in contrast to in 0.9 M solutions in which they were spherical. Similar pattern occurred again at pH 7.5 in ST solutions. However, aggregators had a less length-to-radius ratio compared with the one at pH 5.5. When pH rose to 9.5, in solutions of heating gelation with 0.1 M salt aggregators had less a length-to-radius ratio than in control solutions. And further

concentrating salt led the shape of aggregator to spherical.

Generally, the radius of gyration of aggregator in HS solutions is larger than in control solutions and solutions of heating gelation respectively. However, the corresponding apparent molecular weight of aggregator is not so. Only at pH 7.5 and 0.9 M, this value in HS solutions was larger than the one in two other types of solutions. This observation hints the external flow assists protein molecules affinity to aggregator along the particular direction and facilitates the dissolution of protein molecules in other areas of aggregator surface. In other words, compared with an aggregator in control solutions and solutions of heating gelation, the one in HS solutions has large ratio of  $R_g/R_h$  (Fig. 4c). It is true but at high pH of 9.5 and high salt concentration ( $\geq 0.5$  M), in which this ratio is independent of the types of solutions.

The values of  $M_w/R_g^3$  in SHT provide more information of aggregator geometrical properties. At low pH ( $\leq 7.5$ ), this value was almost indistinguishable between in solutions of heating gelation and in HS ones but at pH 7.5 and 0.9 M, in which an aggregator was more compact in solutions of heating gelation than the one in HS ones. However, with salt concentrated the relative compactness of aggregator in solutions of heating gelation and HS solutions changed at pH 9.5. At 0.1 M, the compactness of aggregator in both types of solutions (heating gelation and HS) was same. But at 0.5 M, an aggregator in solutions of heating gelation presented more compact while the one in HS solutions did at 0.9 M.

### 3.4 Effects of shear on the complex viscosity

The time/temperature evolution of rheological properties in myofibrillar protein solutions opens an avenue to probe protein molecule structure changes during the gelation process [45]. However, as shear was generated by rotational movement, the routine rheological properties, such as the storage modulus ( $G'$ ) and loss modulus ( $G''$ ), are difficult to assess using the shear-treatment method. An alternative means to evaluate a solution's rheological properties uses the

complex viscosity  $h^*$ , as variation in this parameter can reflect changes in solute composition and structure development [46].

The result of apparent viscosity determination at ( $0.1s^{-1}$ ;  $1^\circ C\ min^{-1}$ ) is unique with the pattern of reduction, enhancement and small fluctuation. The corresponding gel formation process might involve protein denaturation, gel growth, and structure reformation, resulting in a product with the peculiar geometrical shape depicted in Fig. S1a.  $h^*$  fluctuation may come from the linear geometrical structure formation with the cooperation effect of size increasing and the hydrophobic feature shifting as additional protein molecules join the linear gel (Fig. S1a, c).

Regardless of heating rate, low shear rate in myofibrillar protein solutions was generally associated with high  $h^*$  (Fig. 5). Since polymer solution viscosity is affected by the volume of solid particles, high viscosity indicates a loose structure with low shear rate. At low shear rate ( $<1s^{-1}$ ), solutions with low heating rate ( $1^\circ C\ min^{-1}$ ) have greater  $h^*$  than those at high heating rate ( $5^\circ C\ min^{-1}$ ). But as shear rate increased to  $10s^{-1}$ , the relative positions between solutions treated by the two heating rate scenarios changed, suggesting that heating rate affected gel structure.  $h^*$  reduced during the initial heating period (with the exception of  $10s^{-1}$ ,  $1^\circ C\ min^{-1}$ )—an observation consistent with Egelandsdal et. al. [45], who reported at  $\sim 46^\circ C$  the myosin subfragment-1 denatured to form a 3D network. At lower temperatures, with heating, more and more hydrophobic residues exposure to solution due to the protein molecule conformation change, reducing  $h^*$  of the solution [47]. Furthermore, the  $h^*$  reduction suggested the process of protein molecule aggregation was rare in this temperature range. An intriguing question arises from the results of Landoll [47], in which  $h^*$  first increases, then decreases, as the hydrophobic content of the target polymer increases. Additionally, our results suggest that solutions containing native proteins have greater  $h^*$  than solutions containing proteins of other conformational states. The reason for this phenomenon is not clear.

The temperature ranges over which  $h^*$  reduced depended on shear rate. As shear rate increased (at  $1^\circ\text{C min}^{-1}$  heating rate) the rate of reduction in  $h^*$  increased. However, minimum  $h^*$ s at different shear rates occurred at almost the same temperature, suggesting this temperature marked the onset of protein molecule conformation change and was independent of shear rate in myofibrillar protein solutions. The occurrence of molecule aggregation depended solely on temperature; it was independent of protein conformation at low heating rate ( $1^\circ\text{C min}^{-1}$ ). In contrast, at the higher heating rate ( $5^\circ\text{C min}^{-1}$ ), minimum  $h^*$ s occurred at both high temperature and high shear rates. An intriguing phenomenon occurred at  $10\text{s}^{-1}$  and  $1^\circ\text{C min}^{-1}$ , in which  $h^*$  evolution contained the reduction part and fluctuation period. This pattern indicated the failure of a 3D network during heating, supported by Fig. S1c. Results at  $0.1\text{s}^{-1}$  ( $5^\circ\text{C min}^{-1}$ ) and  $1\text{s}^{-1}$  ( $1^\circ\text{C min}^{-1}$ ) are also of interest, as following reduction,  $h^*$  continued to increase. In accordance with aforementioned theory, the 3D network continued to grow after the initial period of protein denaturation, supported by Fig S1b and d, gels with large volume. Our results suggest that heat rate has a greater influence on protein gelation than does shear rate.

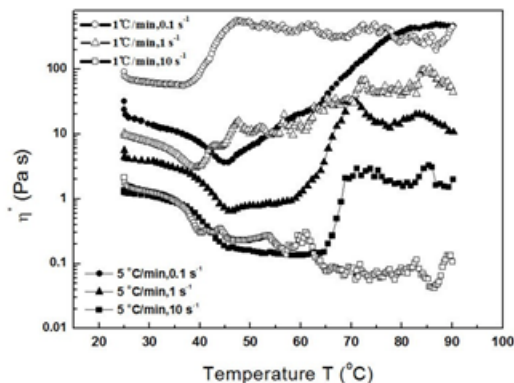


**Figure 5.** Apparent viscosities of myofibrillar protein solution at different temperatures ( $1^\circ\text{C min}^{-1}$  (open symbol),  $5^\circ\text{C min}^{-1}$  (solid symbol)) and shear rates ( $0.1\text{ s}^{-1}$  (circle),  $10\text{ s}^{-1}$  (square)).

### 3.5. Effects of shear on water distribution in gel

Gel water contents reveal positive relationships between WHC, pH and KCl concentration (Table 3). All trends were independent of gelation method.

Generally, gel water contents formed from solutions treated by HS were higher than those of gels formed by heating gelation. At  $0.1\text{ M KCl}$ , differences between the WHC of these two gel types decreased with increasing pH. However, at  $0.5\text{ M KCl}$ , the difference was greatest in three salt concentrations. At  $0.9\text{ M KCl}$  and pH 5.5, the WHC was greatest for gels formed by heating gelation. The difference between the WHC of these two gel types (HS and heating gelation) disappeared with increasing pH. This observation is crucial because this trend is inconsistent with the aggregator observations and apparent viscosity measurement.

A second parameter used to evaluate WHC is  $T_2$ , obtained using LF-NMR spectroscopy.  $T_2$  can also be used to determine the microstructural properties of a gel [48].

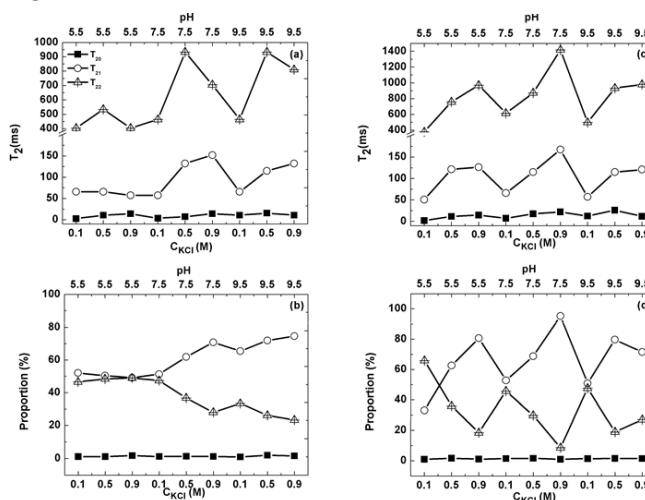


**Figure 6.** Water distributions in gels produced in ST (a, b) and SHT (c, d); a and c show the decay times of three types of water molecules in gels, determined using low-field nuclear magnetic resonance spectroscopy; b and d show area distributions of these three types of water molecules in gels.

Figs. 6a and c illustrate how the  $T_2$  values of a gel formed using simultaneous heating and shearing are usually larger than those of a gel formed using heating alone. A large  $T_2$  implies that the corresponding proton is less restrained and has more freedom [49]. Exposure of hydrophilic residues to the solvent is the main factor restricting proton movement in water for

$T_{20}$  measurements, while the effect of a confined space is the main factor reducing  $T_{21}$  and  $T_{22}$ . Therefore, simultaneous heating and shearing reduces the hydrophilic residue content around the gel surface, but the spaces inside protein molecules and gels are large. Figs. 6b and d show the water contents corresponding to each type of water molecule. Although the contents of type 1 water molecules with  $T_{20}$  are similar in the two types of gel, the contents of the other two types of water molecule depend on solution conditions. A likely explanation for this is that protein or protein aggregators in HSs prefer hydrophilic patch exposure to solutions with high polarization.

### 3.6. Hydrophobic interactions during protein gelation

The development of a 3D protein structure involves two competing steps [50]: 1) single protein molecule denaturation, and 2), bond formation between protein molecules. The driving force causing attraction between neighboring protein molecules that enables them to stay together long enough for bond formation needs to be better understood. Bond distances in a protein gel are comparable to or less than the minimum required for intermolecular interactions, and the bond orientation is specific; accordingly, development of a protein gel 3D structure should be similar to protein crystal nucleation and growth processes. However, the difference between the speeds of these two processes is several orders of magnitude. As such, the driving force in protein gelation should be greater than the intermolecular forces normally present in protein solutions, such as Van der Waals and double-layer forces [38]. In gelation, a protein molecule is first denatured, with hydrophobic patch exposure during this step creating a hydrophobic force. Theoretical simulations and experimental results sug-

gest hydrophobic forces are driving forces in gelation [38].

Any factor that affects a hydrophobic force could be used to tune protein gelation. An edible solvent or glycerin that significantly modifies interactions between water molecules and the host protein molecule could be used to tune a hydrophobic force, and therefore modify the protein gelation process. Another potential agent could modify the evolution of protein denaturation or change the speed of this process, such as, for example, calcium ions that affect myofibrillar protein gelation [51].

In Figs. 6a and b,  $T_{20}$  and its proportion are almost constant without significant difference throughout the measured range. Since  $T_{20}$  and its proportion represent the polarity of exposure hydrophilic residue and its area, respectively, the aforementioned observation suggests that the polarity and area of exposure of hydrophilic residue are almost the same in all studied cases. This conclusion implies that protein molecules in all cases undergo similar evolution in molecular conformation. As hydrophobic interactions drive protein gelation, they are independent of KCl concentration and pH in Humboldt squid myofibrillar protein solution. It is well known that ion concentration can reduce the number of water molecules around protein molecules [52]. However, KCl concentration did not influence hydrophobic interactions, suggesting at least some water did not strongly interact with host protein molecules. This result is corroborated by the picture of water structure around a lysozyme molecule, in which three layers characterized by the inside water structure exist: the compact, loose, and buck water layers, from the host molecule to the buck solution [53].

**Table 3:** Water-holding capacity (WHC) of myofibrillar protein gels.

WHC	$C_{KCl}$ (M)					
	0.1		0.5		0.9	
pH	ST	SHT	ST	SHT	ST	SHT
5.5	40.7±5.3 <sup>ax</sup>	55.3±3.5 <sup>bx</sup>	47.3±5.5 <sup>ax</sup>	49.9±8.5 <sup>ax</sup>	59.1±5.1 <sup>ax</sup>	53.7±2.0 <sup>bx</sup>
7.5	44.3±7.8 <sup>ax</sup>	62.5±6.0 <sup>by</sup>	53.8±5.0 <sup>ay</sup>	63.8±2.7 <sup>by</sup>	58.4±4.5 <sup>ax</sup>	64.5±7.9 <sup>ay</sup>
9.5	66.7±4.2 <sup>ay</sup>	73.8±7.9 <sup>bz</sup>	69.7±8.3 <sup>az</sup>	74.5±8.8 <sup>az</sup>	72.6±7.9 <sup>ay</sup>	74.3±4.4 <sup>az</sup>

<sup>a-b</sup> Within each pair (ST vs. SHT), means with different superscripts are significantly different ( $p < 0.01$ ).

<sup>x-z</sup> Within columns, means with different superscripts are significantly different ( $p < 0.01$ ).

#### 4. CONCLUSION

The effects of shear on gelation in solutions of myofibrillar protein extracted from Humboldt squid were investigated. Generally, shear during gelation favored formation of a gel with high water content and compact structure, and exposure of a high number of hydrophobic patches inside the gel. High pH was beneficial to gel mechanical properties, while the influence of KCl concentration on gel properties depended on pH. The similarity between protein crystallization and gelation processes suggests that hydrophobic interactions are driving forces in the process of gelation.

Our results confirm the feasibility of assessing structural changes ranging from single molecules to 3D networks in the gelation process via the apparent viscosity measurement in food protein systems, differentiating them from the routine biophysical targets due to complex compositions with the strong interactions between them [54]. Both heating rate and shear rate can be manipulated to generate gels with diverse geometrical structures on scale ranging from micrometers to millimeters (Figs. S1, S2). However, predicting combinations of parameters to generate gels with ideal physical properties is not yet possible given unpredictable factors, such as the confinement of 3D network [55].

Our results provide baseline data on the effects of shear on food protein gelation, and could therefore enable the development of surimi processes via optimization of protein gelation using shear. Identification of the forces driving protein gelation might shed further light on developing areas of research, such as neurological disease treatment, and new materials development based on protein aggregation.

#### SUPPORTING INFORMATION

Myofibrillar protein extraction; gelation of myofibrillar protein extracted from Humboldt squid, Fig. S1; scanning electron microscopy (SEM) observations; Figure S2.

#### ACKNOWLEDGEMENTS

This work was supported by grants from the National Natural Science Foundation of China (31171713, 31701650), the Foundation of Food Science and Engineering, the Most Important Discipline of Zhejiang Province (JYTsp20142014), The Natural Science Foundation of Zhejiang Province (LY17C200004).

#### CONFLICTS OF INTEREST

There are no conflicts to declare.

#### REFERENCES

- [1] I. B. Bekard, P. Asimakis, J. Bertolini and D. E. Dunstan, *Biopolymers* 95, 733-745 (2011). PMID:21544798
- [2] E. D. Stasio and R. D. Cristofaro, *Biophys. Chem.* 153, 1-8 (2010). PMID:20797815  
[View Article](#) [PubMed/NCBI](#)
- [3] J. Jaspe and S. J. Hagen, *Biophys. J.* 91, 3415-3424 (2006). PMID:16891374  
PMCID:PMC1614479 [View Article](#) [PubMed/NCBI](#)
- [4] L. Ashton, J. Dusting, E. Imomoh, S. Balabani and E. W. Blanch, *Biophys. J.* 96, 4231-4236 (2009). PMID:19450493  
PMCID:PMC2712145 [View Article](#) [PubMed/NCBI](#)
- [5] M. C. Byington, M. S. Safari, J. C. Conrad and P. G. Vekilov, *J. Phys. Chem. Lett.* 7, 2339-2345 (2016). PMID:27267087 [View Article](#) [PubMed/NCBI](#)
- [6] M. C. Byington, M. S. Safari, J. C. Conrad and P. G. Vekilov, *J. Cryst. Growth* 468, 493-501 (2017). [View Article](#)
- [7] R. Giordano, M. P. Fontana and F. Wanderlingh, *J. Chem. Phys.* 74, 2011-2015 (1981). [View Article](#)
- [8] S. E. Charm and C. J. Lai, *Biotechnol. Bioeng.* 13, 185-202 (1971). PMID:4931754  
[View Article](#) [PubMed/NCBI](#)
- [9] J. E. Sadler, *Annu. Rev. Med.* 56, 173-191 (2005). PMID:15660508 [View Article](#) [PubMed/NCBI](#)
- [10] A. Lazidis, R. D. Hancocks, F. Spyropoulos, M. Kreuss, R. Berrocal and I. T. Norton, *Food Hydrocolloids* 53, 209-217 (2016). [View Article](#)
- [11] H. Yamanaka, M. Matsumoto, K. Hatae

- and H. Nakaya, NIPPON SUISAN GAKKAISHI 61, 612-618 (1995). [View Article](#)
- [12] G. Y. Sánchez-Brambilia, G. Alvarez-Manilla, F. Soto-Cordova, B. G. Lyon and R. Pacheco-Aguilar, J. Aquat. Food Prod. Technol. 13, 55-67 (2004).
- [13] J. A. Cortés-Ruiz, R. Pacheco-Aguilar, M. Elena Lugo-Sánchez, M. Gisela Carvallo-Ruiz and G. García-Sánchez, Food Chem. 110 (2), 486-492 (2008). PMID:26049243 [View Article](#) [PubMed/NCBI](#)
- [14] M. C. Gómez-Guillén, P. Montero, M. T. Solas and A. J. Borderías, J. Agric. Food Chem. 46, 3440-3446 (1998). [View Article](#)
- [15] R. Zhang, R. Zhou, W. Pan, et al., Food Chem. 215, 256-262 (2017). PMID:27542474 [View Article](#) [PubMed/NCBI](#)
- [16] L. Whitmore and B. A. Wallace, Nucleic Acids Res. 32, W668-W673 (2004). PMID:15215473 PMCid:PMC441509 [View Article](#) [PubMed/NCBI](#)
- [17] U. K. Laemmli, Nature 224, 680-685 (1970). [View Article](#)
- [18] B. H. Zimm, J. Chem. Phys. 16 (12), 1093-1099 (1948). [View Article](#)
- [19] D. Eisenberg and D. Crothers, Physical Chemistry: with Applications to Life Sciences. (The Benjamin/Cummins, Menlo Park, 1979), pp
- [20] CRC Handbook of Chemistry and Physics. (2005).
- [21] W. Pan, O. Galkin, L. Filobelo, R. L. Nagel and P. G. Vekilov, Biophys. J. 92, 267-277 (2007). PMID:17040989 PMCid:PMC1697867 [View Article](#) [PubMed/NCBI](#)
- [22] S. W. Provencher, Comput. Phys. Commun. 27 (3), 213-324 (1982). 90173-4 [View Article](#)
- [23] S. W. Provencher, Comput. Phys. Commun. 27 (3), 229-242 (1982). 90174-6 [View Article](#)
- [24] P. R. Kuhn and E. A. Foegeding, J. Food Sci. 56 (3), 789-791 (1991). [View Article](#)
- [25] H. C. Bertram, A. H. Karlsson and H. J. Andersen, Meat Sci. 65, 1281-1291 (2003). 00038-X [View Article](#)
- [26] J. P. Renou, t. I. J. Kopp, P. Gatellier and G. Monin, Meat Sci. 26, 101-114 (1989). 90033-8 [View Article](#)
- [27] T. Giesa, C. C. Perry and M. J. Buehler, Biomacromolecules 17, 427-436 (2016). PMID:26669270 [View Article](#) [PubMed/NCBI](#)
- [28] I. B. Bekard, P. Asimakis, J. Bertolini and D. E. Dunstan, Biopolymers 95:, 733-745 (2011). PMID:21544798
- [29] M. G. Noro and D. Frenkel, J. Chem. Phys. 113, 2941 (2000). [View Article](#)
- [30] M. Muschol and F. Rosenberger, J. Chem. Phys. 107 (6), 1953-1962 (1997). [View Article](#)
- [31] J. R. Lakowicz, Principles of Fluorescence Spectroscopy, 3rd ed. (Springer Science + Business Media, LLC, New York, NY, USA, 2006). [View Article](#)
- [32] W. Lin, L. Jianrong, P. Weichun, F. Yuying and L. Ang, J. Chin. Inst. Food Sci. Technol. 17, 39-46 (2017).
- [33] J. D. Ferry, Adv. Protein Chem. 4, 1-78 (1948). 60004-2 [View Article](#)
- [34] D. A. McQuarrie, Statistical Mechanics. (University Science Books, Sausalito, CA, 2000).
- [35] T. Dapcevic-Hadnadev, M. Hadnadev, A. Lazaridou, T. Moschakis and C. G. Biliaderis, Food Hydrocolloids 81, 481-489 (2018). [View Article](#)
- [36] N. Chen, C. Chassenieux and T. Nicolai, Food Hydrocolloids 77, 66-74 (2018). [View Article](#)
- [37] H. Yamakawa, Modern Theory of Polymer Solutions. (Haper & Row, New York, 1971). PMCid:PMC285097
- [38] J. N. Israelachvili, Intermolecular and Surface Forces, 3 ed. (Academic Press, San Diego, CA, USA, 2011).
- [39] P. Atkins, Physical Chemistry, 6th ed. (Freeman, New York, 1998).
- [40] J. O. M. Bockris, J. Bowler-Reed and J. A. Kitchener, Trans. Faraday Soc. 47, 184-192 (1951). [View Article](#)
- [41] W. Pan, P. G. Vekilov and V. Lubchenko, J. Phys. Chem. B 114, 7620-7630 (2010). PMID:20423058 [View Article](#) [PubMed/NCBI](#)
- [42] A. Fersht, Structure and Mechanism in Protein Science. (W. H. Freeman, New York, 1999).
- [43] R. Zhou, Q. Ni, W. Lin, et al., J. Chin. Inst.

- Food Sci. Technol., 32–39 (2015).
- [44] W. Schärfl, *Light Scattering from Polymer Solutions and Nanoparticle Dispersions*. (Springer, Leipzig, Germany, 2007).
- [45] B. Egelandstal, K. Fretheim and K. Samejima, *J.Sci. Food Agric.* 37, 915-926 (1986). [View Article](#)
- [46] J. M. Dealy and J. Wang, *Melt Rheology and its Applications in the Plastics Industry*, 2nd ed. (Springer Springer Dordrecht Heidelberg New York London, 2013). PMID:PMC4060279 [View Article](#)
- [47] L. M. Landoll, *J. Polym. Sci. Part A: Polym. Chem.* 20, 443-455 (1982). [View Article](#)
- [48] M. Han, P. Wang, X. Xu and G. Zhou, *Food Res. Int.* 62, 1175-1182 (2014). [View Article](#)
- [49] H. Yang, M. Han, Y. Bai, Y. Han, X. Xu and G. Zhou, *Meat Sci.* 102, 69-78 (2015). PMID:25553411 [View Article](#) [PubMed/NCBI](#)
- [50] A. Lomakin, D. S. Chung, G. B. Benedek, D. A. Kirschner and D. B. Teplow, *Proc. Natl. Acad. Sci. U. S. A.* 93 (3), 1125-1129 (1996). PMID:8577726 [View Article](#) [PubMed/NCBI](#)
- [51] J. Yongsawatdigul and S. Sinsuwan, *Food Hydrocolloids* 21, 359-367 (2007). [View Article](#)
- [52] S. Shimizu, *Proc. Natl. Acad. Sci. U. S. A.* 101, 1195-1199 (2004). PMID:14732698 PMID:PMC337029 [View Article](#) [PubMed/NCBI](#)
- [53] W. Pan, University of Houston, 2006.
- [54] R. Mezzenga, P. Schurtenberger, A. Burbidge and M. Michel, *Nat. Mater.* 4, 729-740 (2005). PMID:16195765 [View Article](#) [PubMed/NCBI](#)
- [55] D. Lucent, V. Vishal and V. S. Pande, *Proc. Natl. Acad. Sci. U. S. A.* 104, 10430-10434 (2007). PMID:17563390 PMID:PMC1965530 [View Article](#) [PubMed/NCBI](#)

## SUPPORTING INFORMATION

**Myofibrillar protein extraction**

KCl solutions of concentrations 0.5 and 0.9 M were prepared by dissolving the desired amount of KCl powder (which was dried at 100 °C overnight) in the corresponding buffer solutions.

Myofibrillar protein samples were prepared using the procedure described by Hashimoto, Watabe, Kono, and Siro<sup>1</sup>, with minor modifications. The muscle was minced using a meat grinder. A mixture of ground muscle and buffer A (0.02 M Tris-HCl, 0.1 M KCl, pH 7.5,) (1:10, w/v) was homogenized using a tissue homogenizer (Homogenizer T25 basic, IKA, Staufen, Germany) at 9600 rpm. Homogenization was performed in an ice bath to avoid overheating and consequent protein denaturation; five cycles of homogenization for 30 s followed by a 30-s interval were performed. The connective tissues were removed by filtration using two layers of gauze. The filtrate was incubated for 20 min at 4 °C and then centrifuged at 5000g for 15 min at 4 °C (Biofuge Stratos, Thermo Scientific Inc., Belmont, CA, USA). The supernatant was removed and the sediment was suspended in 10 volumes of phosphate buffer B (0.02 M Tris-HCl, 1% Triton, 0.1 M KCl, pH 7.5). This sample was centrifuged at 5000g for 15 min at 4 °C. This procedure was repeated three times. The final pellet (the myofibrillar protein precipitate) was washed with solutions of various pHs and KCl concentrations. The mixtures were centrifuged at 5000g for 15 min at 4 °C (Biofuge Stratos, Thermo Scientific Inc., Belmont, CA, USA). The supernatant was removed and the washing procedure was repeated twice. The pellets were placed in tubes and stored in a refrigerator at 4 °C. All pellets were used within 24 h.

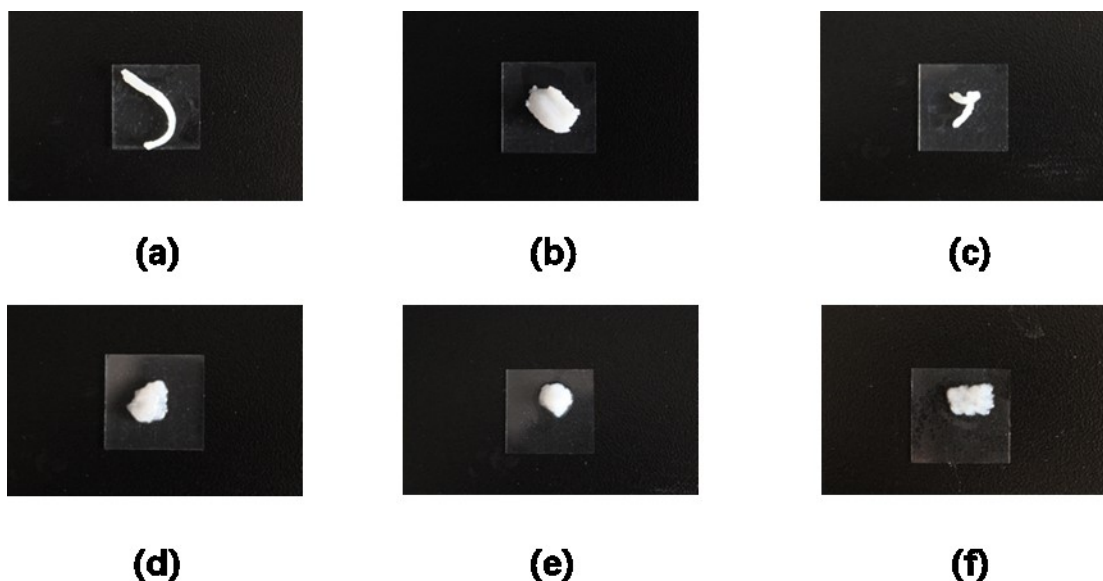


**Fig. S1** The observations of gelation of myofibrillar protein extracted from giant squid. (a) The heating rate is  $1^{\circ}\text{C min}^{-1}$  and the rotation rate is  $0.1 \text{ s}^{-1}$ , (b)  $1^{\circ}\text{C min}^{-1}$  and  $1 \text{ s}^{-1}$ , (c)  $1^{\circ}\text{C min}^{-1}$  and  $10 \text{ s}^{-1}$ , (d)  $5^{\circ}\text{C min}^{-1}$  and  $0.1 \text{ s}^{-1}$ , (e)  $5^{\circ}\text{C min}^{-1}$  and  $1 \text{ s}^{-1}$ , (f)  $5^{\circ}\text{C min}^{-1}$  and  $10 \text{ s}^{-1}$ . The size of cover glass is  $\sim 2 \text{ cm} \times 2 \text{ cm}$ . The detail information for gelation could be obtained in the context.

**Scanning electron microscopy (SEM) observations**

The microstructures of the gels were investigated using SEM. The samples were prepared using the method described by Ma et al.<sup>2</sup>. The gels were cut into cubes ( $1 \times 1 \times 1 \text{ mm}^3$ ) and fixed with 2.5% (w/w) glutaraldehyde solution (Beijing Leagene Biotechnology Inc. Ltd., Beijing, China) overnight. The washed samples were dehydrated using a series of ethanol concentrations (30%, 50%, 70%, 80%, and 95%, and three times with 100%) for 15 min at each concentration. The samples were then freeze-dried and coated with gold. The samples were observed using a Hitachi-1000 instrument (Tokyo, Japan) at an accelerating voltage of 15 kV. ImageJ software (NIH, Bethesda, Maryland, USA) was used to process the SEM images. First, the SEM images were transformed into two-value gray images. The Fractal Dimension and Lacunarity plugins were then used to determine the fractal dimensions of the SEM image based on the box-counting method<sup>31</sup>.

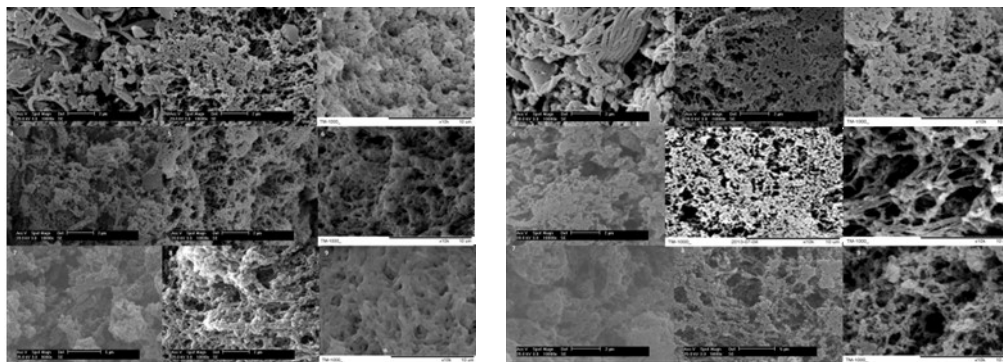


**Fig S2.** SEM images of myofibrillar protein gel (a) without and (b) with shear treatment. Images in top row show gels created at pH 5.5, those in the middle row show gels prepared at pH 7.5, and those in the bottom row show gels prepared at pH 9.5. Images in the left column show gels prepared using 0.1 M KCl, those in the central column show gels prepared using 0.5 M KCl, and those in the right column show gels prepared using 0.9 M KCl.

### Reference

1. K. Hashimoto, S. Watabe, M. Kono and K. Shiro, *Bulletin of the Japanese Society of Scientific Fisheries*, 1979, **45**, 1435-1441.
2. F. Ma, C. Chen, L. Zheng, C. Zhou, K. Cai and Z. Han, *Meat Science*, 2013, **95**, 22-26.
3. T. G. Smith, G. D. Lange and W. B. Marks, *Journal of Neuroscience Methods*, 1996, **69**, 123–136.